

AD-A104 123 MASSACHUSETTS UNIV AMHERST ASTRONOMY RESEARCH FACILITY F/G 4/1
INFRARED EMISSION SPECTROSCOPY OF LOW PRESSURE GASEOUS DISCHARGES--ETC(U)
MAR 81 H SAKAI F1962A-76-C-0087
UNCLASSIFIED UMASS-ARF-80-312 AFGL-TR-80-0355 NL

1 of 1
AD-A104-123

END
DATE FILMED
10-81
DTIC

Y
FILE COPY

AD A104123

AFGL-TR-80-0355

2

LEVEL III
AD91744

INFRARED EMISSION SPECTROSCOPY OF LOW PRESSURE GASEOUS DISCHARGES

Hajime Sakai

Astronomy Research Facility
University of Massachusetts
Amherst MA 01003

March 1981

Final Report
1 October 1975 - 30 September 1980

Approved for public release; distribution unlimited.

AIR FORCE GEOPHYSICS LABORATORY
AIR FORCE SYSTEMS COMMAND
UNITED STATES AIR FORCE
HANSCOM AFB, MASSACHUSETTS 01731

DTIC
ELECTE
S D
SEP 11 1981
D

81 9 11 053

UNCLASSIFIED

SECURITY CLASSIFICATION OF THIS PAGE (When Data Entered)

| REPORT DOCUMENTATION PAGE | | READ INSTRUCTIONS BEFORE COMPLETING FORM |
|---|----------------------------------|---|
| 1. REPORT NUMBER AFGL-TR-80-0355 | 2. GOVT ACCESSION NO. 1D-A104 | 3. RECIPIENT'S CATALOG NUMBER 123 |
| 4. TITLE (and Subtitle) INFRARED EMISSION SPECTROSCOPY OF LOW PRESSURE GASEOUS DISCHARGES. | | 5. TYPE OF REPORT & PERIOD COVERED Final 31 Oct 75 to 30 Sep 80 |
| 7. AUTHOR(s) Hajime/Sakai | | 6. PERFORMING ORG. REPORT NUMBER UMASS-ARF-80-312 |
| 9. PERFORMING ORGANIZATION NAME AND ADDRESS Astronomy Research Facility University of Massachusetts Amherst MA 01003 | | 10. PROGRAM ELEMENT, PROJECT, TASK AREA & WORK UNIT NUMBERS 61102F 2310G413 |
| 11. CONTROLLING OFFICE NAME AND ADDRESS Air Force Geophysics Laboratory Hanscom AFB, Massachusetts 01731 Monitor/Alastair Fairbairn/CPR | | 12. REPORT DATE March 1981 |
| 14. MONITORING AGENCY NAME & ADDRESS (if different from Controlling Office) | | 13. NUMBER OF PAGES 50 |
| | | 15. SECURITY CLASS. (of this report) Unclassified |
| | | 16a. DECLASSIFICATION/DOWNGRADING SCHEDULE |
| 16. DISTRIBUTION STATEMENT (of this Report) Approved for public release; distribution unlimited. | | |
| 17. DISTRIBUTION STATEMENT (of the abstract entered in Block 20, if different from Report) | | |
| 18. SUPPLEMENTARY NOTES | | |
| 19. KEY WORDS (Continue on reverse side if necessary and identify by block number) Emission spectra Infrared N ₂ O Fourier spectroscopy Nitrogen NO Gaseous discharge OH CO ₂ Oxygen NH CO | | |
| 20. ABSTRACT (Continue on reverse side if necessary and identify by block number) Our study conducted on the infrared emission of atmospheric atoms and molecules is summarized in this report. In addition, the nitrogen emission study which was conducted in the final phase of the contract is reported. The singlet transition $\text{w}^1\Delta_u - \text{a}^1\pi_g$, which was partially observed by McFarlane, was fully observed and its band constants were determined. The only vibrational transition detected for the triplet transition $\text{W}^3\Delta_u - \text{B}^3\pi_g$ was the (2-0) band. We failed to detect other members which belong to the same transition. | | |

The work conducted for this contract research can be summarized as the infrared emission spectroscopy study of various atmospheric species; in particular, emphasis on nitrogen's molecular bands. In the course of our study, we found that the vibrational progressions of the $W\ ^3\Delta_u^-$ $B\ ^3\pi_g$ transition did not conform to the assignment made by Saum and Benesch. The band features at 2460 cm^{-1} and at 2740 cm^{-1} , assigned as the (3-1) and (4-2) bands of the W-B transition by Saum and Benesch, were quite different in their fine structure from the triplet structure. We found it rather difficult to explain why our data have the intensity pattern so different from the ordinary vibrational progression of the N_2 transitions involved. Our experiment was intended to study the infrared radiation background produced in the atmosphere of 0.1 torr excited by the electrons of 20-30 ev. We expected to obtain the infrared emission from a large glow discharge column in a well controlled environment. The unexpected abnormal behavior observed in the nitrogen infrared emission made us realize that the study demands more extensive work.

This final report is divided into two major independent parts. The first part gives a survey description of the infrared emission produced by various atmospheric species. In the second part, the study conducted on the nitrogen emission and some conclusions reached by the study are given. The nitrogen emission in infrared is the most important part of the upper atmospheric radiative background.

Before these two parts, we devote a short section to describe the history of our effort during the entire contract period. All statements in this part are given without specific references, as their primary purpose is to provide an overview of our study.

Our study effort underwent various stages of progress. It was started principally by Peter Hansen under the direction of John Strong. During the years, the program had several changeovers in the principal participants. Each participant made a specific contribution on a specific effort during a specific phase. The author feels that the contribution by each participant should be properly acknowledged. The following description is for that purpose.

The work covered in this contract period may be divided into three phases. The first two years was a period for developing a large glow discharge source to which the infrared emission study was performed. Most of the work in that period was carried out by Peter Hansen. Our large 30-meter long absorption cell was converted to a discharge source by installing the central electrode. Our Scientific Report I summarizes our effort during the first phase. At the end of this period, Hajime Sakai joined into the study effort. His primary function was to direct the research effort of the contract. The second phase started during the summer of 1977. The major effort during the second phase was to implement the technique of Fourier spectroscopy for our experimental setup. Rapid progress of the work finally came after the LSI/11 computer was implemented into the experimental setup during the winter of 1978. We owed this progress very much to the software effort of Mark Esplin. Most of the software programs which were written for the LSI/11 to accomplish the control of the interferometer operations and the recording of the interferogram data were developed during this phase. The softwares for the data transmission to the central site CYBER system from the LSI/11 system via the MODEM were simultaneously developed during this phase. The basic Fourier

transformation routines used in the data process were those originally developed by Sakai. They were later, in 1980, revised by Esplin, resulting in improvement of the computation efficiency by a factor of $2 \sim 4$. The interferometer was modified by Hansen to accommodate the InSb detector operation. The second phase was completed during the winter of 1978-79, followed by the spectral data measurements of all atmospheric species. Our effort and progress during the second phase were summarized in the Scientific Report II. The effort for extending the spectral measurement to the lower wavenumber region produced no success. A low level of the infrared emission in the lower wavenumber region and a low sensitivity of the HgCdTd detector required scanning the interferometer at a speed much slower than the present instrument can allow. We gave up extending the spectroscopy to the 1000 cm^{-1} region after several months of an intensive effort. The third and final phase was a period for the spectral analysis of the data.

In addition to those people mentioned above, Ronald Johansson, William Dalton, and Martti Peltola were engaged in the data measurement.

| | |
|---------------------------|-------------------------------------|
| Accession For | |
| NTIS GRA&I | <input checked="" type="checkbox"/> |
| DTIC TAB | <input type="checkbox"/> |
| Unannounced | <input type="checkbox"/> |
| Justification | |
| By _____ | |
| Distribution/ | |
| Availability Codes | |
| Dist | Avail and/or Special |
| A | |

I. INFRARED EMISSION OF ATMOSPHERIC ATOMS AND MOLECULES

Introduction

Recently, in parallel with the advent of infrared technology, various study efforts revealed the atomic and molecular infrared emission features which were poorly known in the past. In two specific areas of the observational studies, one for the atmospheric interest and another for the astrophysics interest, the spectroscopic data of the infrared emission are obtained for situations which were considered impossible a decade ago. Most of the emission data currently obtained in field observations are those of a relatively low spectral resolution, resulting in a difficult task for the identification of the spectral feature found in the data. A primary objective in the field observation study is concerned with physical and chemical processes involved in the emission mechanism. It cannot be achieved unless a proper identification can be assigned to the observed spectral feature. Under the circumstances where the field data are provided with a spectral resolution insufficient for producing a clear spectral identification, a laboratory spectroscopic study on the candidate atomic and molecular infrared emission provides worthwhile assistance to the analysis effort. Our study effort was made in part to fulfill the need called for in such a circumstance. We collected the data on the infrared emission feature of atmospheric species, atoms and molecules, with a moderate spectral resolution using the technique of Fourier spectroscopy and studied them.

The primary interest of our study was focused on the region of the upper atmosphere above 60 km, where the pressure remains below 1 torr.

The infrared emission generated by the electrons of 20-30 ev exciting the atmospheric molecules was our main study subject. Our basic experimental approach to the study was twofold: (1) by forming a large electric glow discharge column, the infrared photons of various atmospheric species were produced in a large quantity; and (2) by using Fourier multiplex spectroscopy, the efficiency of collecting the generated infrared photons was optimized.¹ By combining these two factors, we were able to enhance the detection sensitivity to such a level that only 15 minutes observation time is required to cover the entire InSb spectral range ($1800 \sim 7800 \text{ cm}^{-1}$) with a spectral resolution of 1 cm^{-1} .

An atomic or a molecular transition falls into the infrared range if the upper and the lower state of the transition are separated by an infrared frequency. An electric dipole transition of a homonuclear diatomic molecule takes place from a vibrational-rotational level of an electronic state to another level which belongs to a different electronic state. Since in general the stable diatomic molecules have their first electronic excited state a few electron volts above the ground state, the infrared emission of a homonuclear diatomic molecule is produced by an electronic transition which does not involve the ground state. It must take place between two different electronic excited states. The infrared atomic emission occurs in a similar situation. It takes place between two excited states which are separated by the infrared energy. These two situations for the electronic transitions contrast to the normal infrared transition which is found either in a heteronuclear or in a polyatomic molecule. It involves a vibrational-rotational transition within the same electronic state, usually within the ground

electronic state.

Experimental Setup

A central feature of our experimental setup is a 30-meter long, 1-meter diameter cylinder used as a container of the glow discharge source which is formed between a 12-meter long central electrode and the external wall as shown in Fig. 1. An a.c. 60 Hz voltage of up to 1000 V is applied between the electrodes, activating the discharge. The interferometer accepts the infrared radiation through a KBr lens placed at the exit port of the discharge source. The interferogram signal is detected by an InSb detector housed in a liquid nitrogen dewar. The path difference is monitored by the interference fringe signal of the HeNe cw laser lines 6328 \AA (air wavelength). The detector output is properly ac-amplified, synchronously demodulated, integrated and finally converted to a digital signal by an analog-to-digital converter, which is triggered by the zero crossing position of the laser interference fringe reference signal. The digitized interferogram signal is then recorded on a mass storage device (a floppy disk) under the control of an LSI/11 minicomputer. After completion of the interferogram measurement, the interferogram data is post-processed using our central site large-scale computer, CDC CYBER system, for the Fourier transformation, etc.

The optical cell which is used to house our glow discharge source is generally known as the "Pfund" cell.² The discharge column formed between the electrodes is seen thrice along the optical path, thus forming an equivalent 36-meter long discharge column. The discharge region extends only 1/3 of the entire cell length, leaving 2/3 of the

cell a discharge-free space. This apparent disadvantage created by the discharge-free region is a blessing in disguise from the experimental point of view, since it prevents the mirror contamination caused by the electron bombardment.

An important parameter which controls our glow discharge is the excitation energy released to the atoms and the molecules. A rough estimate of the excitation energy can be obtained in the following way. The electric field in the cell is given as a function of a distance r (measured from the center) by

$$E = \frac{V}{r(\ln \frac{b}{a})} , \quad (1)$$

where V is the electric potential applied between the electrode of radius a and the wall of radius b . The electrons pick up their energy under the applied electric field and lose it when they collide with a molecule or an atom. The loss of energy occurred at the collision turns into the energy for exciting the collision partners, for our case either molecule or atom. The energy loss suffered at the collision is usually re-supplied between collisions. The mean free path $\langle x \rangle$ of the electrons, i.e., the mean distance between the successive collisions, is generally characterized by

$$\langle x \rangle = \frac{1}{n\sigma} \quad (2)$$

where n is the number density of the colliding molecules and σ a quantity called the collision cross-section. If an electron moves parallel to the field, it gains its energy by $e\langle x \rangle E$, which is calculated by

$$\epsilon = e\langle x \rangle E = \frac{eVp_0}{r(\ln \frac{b}{a}) N_c \rho \sigma} \quad (3)$$

for the gas pressure of p . In this expression, N_0 is the number density at the standard pressure p_0 . It is seen that the excitation is the highest in the vicinity of the electrode and that it reduces toward the outer wall. For a typical example, we can assume $\sigma = 10^{-16} \text{ cm}^2$, $V = 1000$ volts, and $n = N_0 P/p_0 = 7.07 \times 10^{15}$ for $p = 0.2$ torr. The field at $r = 30$ cm is about 13 V/cm, while the mean free path is about 1.4 cm. The energy gain per collision in the area at $r = 30$ cm would reach $18 \text{ ev} = 145000 \text{ cm}^{-1}$. In reality, the cross-section σ varies dependent on the electron energy and the electrons may lose only a part of their energy by the inelastic collision process. Nonetheless, the value estimated above for the excitation energy agreed well with the experimental data obtained. In the glow discharge of oxygen, for example, observed are many infrared atomic oxygen lines which are produced in transition between two highly excited atomic levels. By identifying the levels involved for the observed infrared atomic OI lines, we estimated the excitation energy in our glow discharge generally reaching a level of 20 ev. Even though some excitations may exceed the value by a substantial degree, it is safe to assume that a majority of the infrared photons observable in our experiment are indeed generated in the processes which require an excitation energy of about 20 ev or less.

One thing noticed is that the excitation is very sensitive to the gas pressure. Once the gas pressure is above 0.5 torr, the glow discharge which is indicative of transitions between the electronic states is confined to the vicinity of the electrodes, leaving a dark space elsewhere. For heteronuclear diatomic molecules, the infrared emission does not necessitate the electronic transition. An absence

of the visible glow discharge does not eliminate a possible infrared emission. However, for homonuclear molecules, the visible glow discharge which usually indicates a presence of the electronic transitions to the ground state is necessary to produce infrared transition.

The glow discharge is run at 60 Hz a.c., obtained from the ordinary 60 Hz power, through a step-up transformer. D.C. voltages failed to produce a stable glow discharge. The central electrode is usually water-cooled.

The spectrum shown in Fig. 2 is a typical result produced by a glow discharge in 0.1 torr of air. Identifiable molecular features in the spectrum are NO, N₂, CO, CO₂, N₂O, OH, NH, and NO₂. The atomic features contain O and N. Each spectral feature of these species as well as of others were studied by observing the infrared glow discharge emissions formed in various gas samples, in addition to those produced in air. Specific mixtures were selected to produce the spectral data necessary for interpreting those features observable in the air discharge.

Emission Spectra of Various Atmospheric Species

The spectrum shown in Fig. 2 was taken with a resolution of approximately 1.0 cm^{-1} . A feature observable between 2000 cm^{-1} and 2400 cm^{-1} consists of CO, N₂O, CO₂ and possibly others. The vibrational fundamental ($\Delta v = 1$) of NO ground state is observable in 1800 cm^{-1} , in the lowest frequency range covered by the InSb detector. A feature which appears as a group of lines at 2500 cm^{-1} consists of many atomic lines.³ The transition frequency of 2470 cm^{-1} corresponds approximately to the energy difference between $n = 4$ and $n = 5$ orbit of the hydrogen-like atoms. Consequently, all atoms contained in the gas samples would

emit infrared lines in a confined spectral region centered at 2470 cm^{-1} .

We found atomic lines of H, N, O and He in this region. The features

observable between 2500 cm^{-1} and 4000 cm^{-1} are of N_2 , NH, OH, and NO_2 .

The features above 5000 cm^{-1} are predominantly those of the N_2 first positive band ($\text{B}^3\pi_g - \text{A}^3\Sigma_u$).⁴ In addition to these molecular features, various atomic lines of H, O, and N spread over the entire InSb region.

The following description provides a survey of the spectral features produced by various atmospheric species. As mentioned above, the glow discharge formed several molecular products which were not found in the original gas samples. The present paper will make no discussions on the formation mechanism of these products. All the measurements were done in integrating the emission intensity using the normal lock-in technique. The formation processes of the glow discharge by-product would be better studied by using the time-resolved spectroscopic technique.

(a) Atomic feature

Hydrogen. The atomic lines of hydrogen were observed in the glow discharge emission of air whenever the sample was moist. Table I lists the atomic H lines observed in the infrared. No molecular transitions of hydrogen were observed in the infrared, even though several known excited electronic states of H_2 are spaced by the infrared frequencies. The atomic hydrogen may have been easily formed because of a low dissociation energy at the ground state ($\text{X}^1\Sigma_g^+$).⁵

The glow discharge emissions were in a great extent affected by admission of hydrogen into the gas sample. There were two notable effects observed in the discharge emission: suppression of the CO vibrational fundamental which would otherwise accompany as a parasitic

Table I

Observed Atomic Hydrogen Lines (cm^{-1})

| n | $\Delta n = 1$ | $\Delta n = 2$ | $\Delta n = 3$ | $\Delta n = 4$ |
|-----|----------------|----------------|----------------|----------------|
| 1 | | | | |
| 2 | | | | |
| 3 | 5331.55 | 7799.29 | | |
| 4 | 2467.75 | 3808.25 | 4616.53 | |
| 5 | | 2148.79 | 2673.39 | 3033.05 |
| 6 | | | | |

emission; and formation of two hydrides, OH and NH.

Oxygen. The atomic lines of oxygen were observed over a wide spectral range. The line position is listed in Table II. It is similar to the hydrogen case where no molecular transitions were observed. The low dissociation energy of the O_2 ground state ($X^3\Sigma_g^+$) contributes to the formation of the atomic oxygen in the glow discharge.⁶ The recent data compiled for the atomic infrared lines by Outred do not contain the oxygen lines below 3819 cm^{-1} .³ Fig. 3 shows the glow discharge emission spectrum of the oxygen gas.

Fig. 4 is a sketch showing the atomic oxygen (O I) energy levels⁷ together with the infrared lines observed in our measurement. The energy of these levels is referenced to the ground state of atomic oxygen ($1S^2(2S)^2(2p)^4\ 3P_2$), which is located at approximately $40,000\text{ cm}^{-1}$ above the molecular O_2 ground state $X^3\Sigma_g^-$. As mentioned above, the estimate made on the electron energy available for the excitation agrees with the excitation energy measured from the observed atomic oxygen lines.

Nitrogen. The infrared emission from the nitrogen gas contains few atomic nitrogen lines. The data compiled by Outred³ contain no NI lines below 5000 cm^{-1} . The feature at 2470 cm^{-1} consists of many lines, as listed in Table III, with their transition identification. Fig. 5 shows the atomic NI emission at 2470 cm^{-1} .

(b) Molecular feature

Nitrogen. The N_2 infrared emission feature fills almost the entire InSb region from 2500 cm^{-1} to 7800 cm^{-1} . There are three distinctive N_2 electronic transitions observable in infrared.⁴ Various vibrational progressions of the first positive band, $B^3\Pi_g - A^3\Sigma_u^-$, are observable

Table II

Observed Atomic Oxygen Lines

| (cm ⁻¹) | Transition |
|---------------------|--|
| 7593.7 | 4s ³ S ⁰ - 3p ³ P |
| 6289.5 | 5d ⁵ D - 4p ⁵ P |
| 5546.9 | 4f ⁵ F - 3d ⁵ D |
| 5479.4 | 4f ³ F - 3d ³ D ⁰ |
| 3918.9 | 6f ⁵ F - 4d ⁵ D |
| 3876.2 | 6f ³ F - 4d ³ D |
| 3819.9 | 8s ⁵ S - 5p ⁵ P |
| 3819.9 | 6g ³ G - 4f ³ F |
| 3770.7 | 4d ⁵ D - 4p ⁵ P |
| 3617.2 | 4p ⁵ P - 4s ⁵ S |
| 3455.4 | 4p ³ P - 4s ³ S |
| 3226.9 | 3d ³ D - 4p ³ P |
| 3021.9 | 5s ⁵ S - 4p ⁵ P |
| 2731.0 | 5s ³ S ⁰ - 4p ³ P |
| 2575.7 | 5f ⁵ F - 4d ⁵ D ⁰ |
| 2532.7 | 5f ³ F - 4d ³ D ⁰ |
| 2477.3 | 5g ⁵ G - 4f ⁵ F |
| 2192.1 | 4p ³ P - 3d ³ D ⁰ |
| 2154.6 | 7g ⁵ G - 5f ⁵ F |
| 2150.5 | 7f ⁵ F - 5g ⁵ G |

Table III

Observed Line Position, Observed and Calculated Intensity
of N I Transition Between $(^3P)5g$ and $(^3P)4f$ Configuration

| J | K' | K'' | Position (cm ⁻¹) | Relative Intensity | |
|---|----|-----|------------------------------|--------------------|------------|
| | | | | Observed | Calculated |
| 0 | 4 | 3 | 2484.9 | 1.0 | 1.0 |
| 1 | 3 | 2 | 2480.6 | 0.8 | 0.7 |
| | 4 | 3 | 2494.1 | 1.0 | 0.9 |
| | 5 | 4 | 2481.9 | 1.3 | 1.2 |
| 2 | 2 | 1 | 2500.3 | 0.5 | 0.4 |
| | 3 | 2 | 2479.0 | 0.6 | 0.6 |
| | 4 | 3 | 2469.6 | 2.7* | 0.8 |
| | 5 | 4 | 2466.7 | 1.3 | 1.1 |
| | 6 | 5 | 2489.3 | 1.4 | 1.4 |

*blended with He I line

over a wide spectral range. The emission spectrum of the N_2/He glow discharge is shown in Fig. 8 to illustrate the band formations. The band centers of $B^3\pi_g - A^3\Sigma_u^-$,⁸ which are indicated in the figure, are listed in Table IV. In contrast to the first positive band, the other two electronic transitions, the Wu-Benesch band $w^3\Delta_u - B^3\pi_g$ ⁹ and the McFarlane band $w^1\Delta_u - a^1\Sigma_g$,¹⁰ do not form a well recognizable vibrational progression. The only observable transition for the $w^3\Delta_u - B^3\pi_g$ band is formed at 3000 cm^{-1} region. The $w^1\Delta_u - a^1\Sigma_g$ band is only observable at 2750 cm^{-1} region where the Wu-Benesch (3-1) band should be found. At 2470 cm^{-1} region where the Wu-Benesch band should be found, the emission feature consisting of a group of the atomic nitrogen lines is observed.

The excitation of the first positive band $B^3\pi_g - A^3\Sigma_u^-$ is found strongly influenced by the discharge condition; its intensity varies over a large range from an undetectably weak level to an extremely strong level. The other two bands which are seen in the low frequency region remained consistently strong. The characteristics of both bands, one at 2740 cm^{-1} and another at 3000 cm^{-1} , remain consistent; a singlet structure was observed for the 2740 cm^{-1} band and a triplet structure of the 3000 cm^{-1} band.

The 2740 cm^{-1} band definitely belongs to the $w^1\Delta_u - a^1\Sigma_g$ transition. Using the observed data shown in Fig. 7, we were able to determine the spectroscopic parameters of this band and found them in a good agreement with those determined from the UV spectral data. The spectroscopic parameters determined by the present study are listed in Table V.

OH. It was found that an enhancement of the hydride emission, OH

Table IV

Observed lines of $v^1\Delta - a^1\pi$ (0-0) transition
and their assignment

| | | | |
|---------|------|---------|------|
| 2652.78 | P 18 | 2731.36 | Q 11 |
| 2660.01 | P 17 | 2732.90 | P 4 |
| 2667.06 | P 16 | 2733.98 | Q 10 |
| 2673.69 | P 15 | 2736.40 | Q 9 |
| 2680.44 | P 14 | 2738.53 | Q 8 |
| 2686.71 | P 13 | 2740.46 | Q 7 |
| 2692.73 | P 12 | 2742.03 | Q 6 |
| 2698.67 | P 11 | 2743.60 | Q 5 |
| 2701.11 | Q 19 | 2744.77 | Q 4 |
| 2704.15 | P 10 | 2745.71 | Q 3 |
| 2706.29 | Q 18 | 2746.46 | Q 2 |
| 2709.67 | P 9 | 2752.85 | R 1 |
| 2710.48 | Q 17 | 2755.38 | R 2 |
| 2714.64 | Q 16 | 2757.64 | R 3 |
| 2714.64 | P 8 | 2759.66 | R 4 |
| 2718.44 | Q 15 | 2761.31 | R 5 |
| 2719.61 | P 7 | 2762.97 | R 6 |
| 2722.02 | Q 14 | 2764.21 | R 7 |
| 2724.37 | P 6 | 2765.26 | R 8 |
| 2725.40 | Q 13 | 2766.20 | R 9 |
| 2728.50 | Q 12 | 2766.71 | R 10 |
| 2728.50 | P 5 | 2767.04 | R 11 |

Table V

The molecular constants determined from the
observed transition of $w\ ^1\Delta_u - a\ ^1\pi_g$

$$T_o' - T_o'' = 2747.15 \text{ cm}^{-1}$$

$$B' = 1.4884 \text{ cm}^{-1}$$

$$D' = .293 \times 10^{-5} \text{ cm}^{-1}$$

$$B'' = 1.6082 \text{ cm}^{-1}$$

$$D'' = .369 \times 10^{-5} \text{ cm}^{-1}$$

and NH, accompanied an increase of the moisture in the sample air. The spectrum shown in Fig. 8 is the glow discharge emission formed in the air mixed with hydrogen. Our experiments indicate that these hydrides are formed with a presence of hydrogen, either atomic or molecular. The presence of H_2O does not seem required for the formation of the hydrides. The infrared OH band was thoroughly studied by Mantz *et al.*¹¹ Our measurement of the OH line position agrees well with them.

NH. A unique feature discovered in our study is the vibrational fundamental transition of the NH free radical in its electronic ground state ($^3\Sigma^-$). The NH lines were observed in the discharge formed in air. It was generally considered that the decomposition process, $NH_3 \rightarrow NH_2 \rightarrow NH$, is the feasible generation mechanism for this free radical. However, the spectra taken with air/ H_2 mixture showed not only a predicted increase in the OH band, but also a striking enlargement in the NH bands. A presence of NH in the glow discharge emission found in the air/ H_2 or N_2/H_2 mixture indicates that the recombination process is undoubtedly responsible for NH formation in these gas samples.

The vibrational rotational transition of NH exhibits a more complex structure than that of the singlet. The NH spectrum in Fig. 9 was taken with a resolution of 0.1 cm^{-1} , which was adequate for spectral analysis. Table VI lists the spectroscopic constants, which are more accurate than those previously measured using the UV data.¹²

NO. The NO band was seen in the air discharge shown in Fig. 2. A complementary relation was observed between the intensity of the NO and the NH bands. With introduction of extra hydrogen to the discharge gas, a weakening of the NO band was observed with an enhancement of the NH band.¹³

Table VI

Spectroscopic constants of NH electronic ground state ($X^3\Sigma$)

| | |
|----------------|--|
| ω_e | 3280.85 cm^{-1} |
| $\omega_e x_e$ | 77.40 cm^{-1} |
| $\omega_e y_e$ | $- .14 \text{ cm}^{-1}$ |
| B_e | 16.674 cm^{-1} |
| α_e | $.650 \text{ cm}^{-1}$ |
| D_e | $17.6 \times 10^{-4} \text{ cm}^{-1}$ |
| β | $- .41 \times 10^{-4} \text{ cm}^{-1}$ |
| λ_0^* | $.911 \text{ cm}^{-1}$ |
| λ_1^* | $- .013 \text{ cm}^{-1}$ |
| γ_0^+ | $- .055 \text{ cm}^{-1}$ |
| γ_1^+ | $.0037 \text{ cm}^{-1}$ |

$$* \lambda = \lambda_0 + \lambda_1 v$$

$$+ \gamma = \gamma_0 + \gamma_1 v$$

The Molecular Emission in $2000\text{ cm}^{-1} \sim 2400\text{ cm}^{-1}$ Region

The feature observed between 2000 and 2400 cm^{-1} is composed of several bands, the CO fundamental, the N_2O $\Delta\nu_3 = 1$ transition,¹³ the CO_2 $\Delta\nu_3 = 1$ transition, and possibly others. The intensity pattern was found critically influenced by the discharge condition. The most persistent feature is the ν_3 transition of N_2O . The excitation of the CO_2 band is affected by the presence of N_2 . In our glow discharge condition, an exact nature of the correlation between the CO_2 and the N_2 excitation is unclear. A detailed study of the emission in this region requires a spectral resolution better than 0.1 cm^{-1} , which is the limit for our experiment.

II. INFRARED EMISSION OF NITROGEN

Nitrogen is a gas of particular interest for atmospheric studies, since it is the major constituent of the earth's atmosphere. Even though extensive data of the nitrogen emission spectra exist, only a handful of studies were made for the infrared emission. Most of the spectroscopic studies on N_2 were conducted in the visible and the uv region.⁴ Some serious discrepancies found between those presently accepted and those observed in our study demand more laboratory study of the infrared N_2 emission. A primary goal of our study was set up to provide unambiguous identification to the infrared emission features of molecular nitrogen.

The potential curves of molecular nitrogen shown in Fig. 10 are taken from reference 4. They are constructed using the data which are presently recognized as acceptable. The lowest excited states are a group of triplet states, consisting of $A^3\Sigma_u^+$, $B^3\Pi_g$, $B'^3\Sigma_u^-$, and $w^3\Delta_u$. In the same energy range of these triplet states, there exist three singlet states, $a^1\Pi_g$, $a'^1\Sigma_u$, and $w^1\Delta_u$. The infrared transitions which were reported in the literature for observations between 1700 and 7800 cm^{-1} are those between the triplet states, the first positive band between $B^3\Pi_g$ and $A^3\Sigma_u^+$ and the Wu-Benesch band⁹ between $w^3\Delta_u$ and $B^3\Pi_g$, and those found by McFarlane¹⁵ which occur between the singlet states, one between $w^1\Delta_u$ and $a^1\Pi_g$ and the other between $a^1\Pi_g$ and $a'^1\Sigma_u^-$.

The first positive band extends over a wide spectral range, not limited in the infrared region. The band center frequencies of the vibrational progression for this band were documented by Dieke and

Heath.⁸ The spectrum shown in Fig. 6 represents an example of the infrared emission data obtained in the present study. Well formed vibrational progressions of $\Delta v = -4$, -3 and -2 are seen in the spectrum. Because the first positive band is the transition which occurs between triplet states, its rotational structure is far more complex than the singlet transition which consists at worst of three branches, P, Q, and R, corresponding to $\Delta J = -1$, 0, and +1. The transition between the $^3\pi_g$ and the $^3\Sigma_u^-$ state would contain nine major branches and eighteen minor (weak) branches. The resulting complexity in the vibrational-rotational transition makes the spectral analysis very difficult for the triplet system. Firstly, the analysis effort requires the spectral data to be well resolved. Secondly, the line assignment requires a time-consuming, painstaking effort. Until the recent work by Effantin, Amiot, and Verges, for the (0-0), (1-0) and (2-0) bands,¹⁶ none of the infrared bands which belong to this transition underwent a thorough spectral analysis. The work by Verges and his co-workers provided a first in the study of this transition, a good set of the spectroscopic constants for the $B^3\pi_g$ and the $A^3\Sigma_u^+$ state.

McFarlane studied the infrared transition of molecular nitrogen in conjunction with the laser emissions.¹⁵ He found several singlet transitions in his laser-type experiment. Those singlet transitions found by McFarlane in the $2700 \sim 3000 \text{ cm}^{-1}$ region are the $w^1\Delta_u - a^1\pi_g$ and the $a^1\pi_g - a' ^1\Sigma_u^-$ transitions. Because the emissions in his experiment were activated in a laser cavity, extremely selective excitations took place. Only 15 lines were observed for the $w^1\Delta_u - a^1\pi_g$ (0-0) band.¹⁰ He noted intensity variation of the transition lines strongly affected by gas pressure.

Subsequent to McFarlane's work, Benesch and his co-workers studied the infrared emission system produced by the electric discharge in O_2 , N_2 , and air.¹⁷ They assigned the band formation observed at 3007, 3734, and 2463 cm^{-1} as the (2-0), (3-1), and (4-2) vibrational progression of the $W\ ^3\Delta_u - B\ ^3\pi_g$ transition. In so doing they synthesized the band profile based on the best available spectroscopic constants of both electronic $W\ ^3\Delta_u$ and $B\ ^3\pi_g$ states. They arrived at their conclusion above based on a good correlation between the observed and the computed spectral profile. Their assignment on the band features observed at these three positions have produced a wide acceptance. Recently, Verges and his co-workers succeeded to complete a spectral analysis on the rotational structure of this 3007 cm^{-1} band feature using the data taken with a superior resolution.¹⁸ Their data established an extremely complex structure typical of the triplet system transition. It would be no question that the 3007 cm^{-1} band feature belongs to the $W\ ^3\Delta_u - B\ ^3\pi_g$ transition.

The band formation of the nitrogen emission in $2400 \sim 3200\text{ cm}^{-1}$ region provided Benesch and his co-workers a central role for the transition assignment. The features found in the spectral region higher than 3200 cm^{-1} overlap very badly with the first position system $B\ ^3\pi_g - A\ ^3\Sigma_u$, thus making the band analysis rather ambiguous. The value presently accepted for the vibrational frequency as well as the electronic term value energy of the $W\ ^3\Delta_u$ state were derived based on the assignment of Benesch *et al.* These basic parameters were in turn used for interpreting the other experimental data.

Recently Cartwright *et al* determined the electronic collision excitation cross-section of the N_2 energy states which are within 15 ev

of the ground state $X^1\Sigma_g^+$.¹⁷ The spectroscopic constants of these electronic states critically affect their analysis. They used those constants determined for various spectroscopic data. For the $W^3\Lambda_u$ state, those determined by Benesch *et al* were adapted. Importance of the term value T and the vibrational frequency ω and others for this state would be clearly realized as the accuracy of these constants affect the analysis a great deal, not only for the $W^3\Lambda_u$ state, but all other states which are in the same energy range.

We took the N_2 emission spectra with a moderate resolution of 0.12 cm^{-1} . The chamber pressure was kept at 0.1 torr, because a stable glow discharge was formed only at this pressure. The collision frequency at 0.1 torr for N_2 was an order of 10^5 s^{-1} . The spectra provided no triplet structure at both band features, 2740 cm^{-1} and 2470 cm^{-1} . We obtained unambiguous identification for both of them, the $W^1\Delta - a^1\pi_g$ transition for the 2740 cm^{-1} feature, and the N I $4f \rightarrow 5g$ transition for the 2470 cm^{-1} feature. The feature at 3000 cm^{-1} indicated a triplet structure. Even though our data lacked sufficient spectral resolution for resolving all rotational structure, they clearly showed the rotational feature no different from the data shown by Verges *et al*,¹⁸ except two distinctive atomic N I lines of the $(^3P)5s \rightarrow (^3P)4p$ transition.

$W^1\Delta_u - a^1\pi_g$

We found that the $W^1\Delta_u - a^1\pi_g$ (0-0) transition is the brightest in the N_2/He discharge emission. Fig. 7 shows a spectrum of this transition taken with a resolution of 0.12 cm^{-1} . The well recognizable features of three branches, P, Q, and R, indicate with no ambiguity that the transition belongs to a singlet system. Unlike the pattern seen by

McFarlane in his optical maser configuration,¹⁰ our spectral data show three well-formed branches. Table IV lists the rotational assignment of the observed lines. As mentioned earlier, we failed to detect a triplet structure anywhere in the 2740 cm^{-1} region. The transition observed consists only of a singlet system. Because of an insufficient spectral resolution, we failed to resolve the Λ doubling.

A result of the spectral analysis conducted on the observed lines is listed in Table IV. The P3 line was removed from our analysis because it blended with the Q9 line. The band head is found at R11. The spectroscopic constants determined in the present analysis are listed in Table V. Our value of ΔT_0 differs from the one given by Lofthus and Krupenie³ by about 0.1 cm^{-1} .⁹ In addition, our observed transition frequencies for the Q lines are generally different by the same magnitude from the ones reported by McFarlane. We believe that our measurement is superior to the previous measurements because the line positions are all calibrated directly with respect to the HeNe laser line at 15789.00 cm^{-1} in vacuum. The conventional technique relies on the inference technique, resulting in less accurate position measurement than that determined by the Fourier technique. The rotational constants of the upper and lower states agree well with the values listed by Lofthus and Krupenie.³ No previous report was found on the distortion constant D.

The Emission Intensity of the Infrared N_2 Bands

Our observation of a single vibration band for both the w-a and W-B transition opened more questions than answers for the emission intensity of various infrared N_2 transitions. Before we proceed to

discuss these questions, we will give the following description for the parameters which are pertinent to our experiment, in order to provide an overall picture of the situation.

The pressure in the glow discharge was maintained at .1 torr for the reason mentioned earlier. The pumping speed was approximately $0.1 \text{ m}^3/\text{sec}$ (200 CFM). With this pumping speed, the gas molecules move from the inlet to the pumping port in an average of 240 seconds, or they diffuse through the discharge space in approximately 90 seconds. A total of 3.3×10^{22} molecules are present in the discharge space, while approximately $.5 \times 10^{16}$ to 2.5×10^{16} electrons, depending upon the current density, are injected to the gas sample for the excitation during a single discharge cycle. Since each electron would undergo an average of 50 excitation collisions, 2.5×10^{17} to 1.25×10^{18} excitation products are formed in $1/120 \text{ sec}$, or 3×10^{19} to 1.5×10^{20} products in a second. A fraction of 10^{-5} to 4×10^{-5} out of the total molecules which are present in the discharge space are excited during a single discharge cycle. These excitation figures correspond to .04 to .20 J of energy deposited on the molecular system for the same time period (or a rate of 5 to 24 W).

The gas samples used in the glow discharge for the N_2 emission study were either N_2 alone or N_2 mixed with He. The He mixture ratio varied from 0% of the total gas sample to 90%. The purpose of mixing He to the gas sample was intended (1) to raise the average electron energy in the excitation, and (2) to control the quenching of the N_2 infrared emission by the ground state molecular nitrogen (X N_2). As mentioned earlier, the current density in the glow discharge condition covered a value of $.5 \times 10^{16}$ to 2.5×10^{16} electrons per a single

discharge period. The spectral data collected for various mixture ratios and current densities exhibited very consistent spectral characteristics of the 2470, 2740 and 3000 cm^{-1} emission features. What we found in these features are: the atomic N I $5p^4 4f$ transition at 2470 cm^{-1} ; the $w^1\Delta - a^1\pi$ (0-0) transition at 2740 cm^{-1} ; and the $w^3\Delta - b^3\pi$ (2-0) transition at 3000 cm^{-1} . If any other members of the vibrational progression which belongs to either transition, the w - a or the w - b , would have ever been excited, they remained below the detection threshold. The b - a transition varied its intensity in a great extent. We failed to find any leading experimental parameters which we think are responsible for control of the b - a transition intensity. Within the range of the mixture ratios and the current densities quoted above, the b - a intensity changed independently from selected discharge parameters for the experiment. At worst case, with the same discharge parameters maintained, we observed its intensity fluctuation of more than 1 order of a magnitude in a few minutes.

Intensity of the w - a Transition

The w - a transition at 2740 cm^{-1} was always very bright. The spectroscopic constants determined for the upper and the lower state of this band were in a good agreement with those obtained from the UV transitions. The molecular potential for these two singlet states, the $w^1\Delta$ and the $a^1\pi$, can be considered accurate for making an intensity estimate within the vibrational progression of this transition with the assumption that the emission is primarily spontaneous. The upper state of this transition, the $w^1\Delta$ state, is populated directly by the electronic collision excitation by $X \rightarrow w$. The population density of various vibrational

levels in the w state is controlled by the Frank-Condon factor for the $w \leftrightarrow X$ transition. The w-a transition in question would be primarily controlled by two factors, the F-C factors for the w-X and those for the w-a. Their calculated values listed in Lofthus and Krupenie³ are based on the molecular potentials which are constructed on the established spectroscopic constants. They can be taken as accurate for our calculation. The intensity ratios among the vibrational bands progressed in the w-a transition are simply calculated by multiplying two F-C factors, one for $X \rightarrow w$ and another for $w \rightarrow a$. Table VIII shows the calculated relative intensity of the bands, the (0-0) through the (6-6). They indicate that either the (1-1) or the (2-2) band would have a similar intensity as the (0-0) band. We expect to observe a well formed vibrational progression of the (0-0), (1-1), and so forth. The theoretical expectation constructed above turned out to be quite contrary to the observed data, indicating a complete failure of our assumption. Recall that McFarlane observed the laser-type emission of the w-a (0-0) transition.¹⁰

There is a high probability that the observed emission is produced by the super-radiant emission process. We must turn our attention for a search of a possible mechanism which leads to the population inversion at the (0-0) transition.

The radiative lifetime of the $w^1\Delta$ state is of order of 10^{-4} sec,²⁰ as shown in Fig. 11. Even though no quenching data are available for this state, they can be expected similar to a value for the collision broadening of the infrared lines by the N_2 molecules. We estimate the vibrational quenching figure of 3×10^{-6} sec at pressure of 0.1 torr by extrapolating the pressure induced collision broadening figure of

Table VII

The band-center and the Frank-Condon factor of the observable infrared transitions ($v' - v''$) for $B\ 3\pi_g - A\ 3\Sigma_u^+$

| <u>v'</u> | <u>v''</u> | <u>Band-Center¹</u> | <u>F.C. Factor²</u> |
|------------------------|-------------------------|--------------------------------|--------------------------------|
| 0 | 5 | 2664 | .008 |
| 1 | 6 | 3075 | .028 |
| 2 | 7 | 3485 | .056 |
| 3 | 8 | 3898 | .081 |
| 0 | 4 | 3986 | .023 |
| 4 | 9 | 4301 | .090 |
| 1 | 5 | 4369 | .066 |
| 2 | 6 | 4751 | .101 |
| 3 | 7 | 5132 | .112 |
| 0 | 3 | 5335 | .067 |
| 4 | 8 | 5512 | .094 |
| 1 | 4 | 5691 | .131 |
| 5 | 9 | 5891 | .060 |
| 2 | 5 | 6045 | .143 |
| 3 | 6 | 6399 | .107 |
| 0 | 2 | 6713 | .166 |
| 4 | 7 | 6751 | .055 |
| 1 | 3 | 7041 | .197 |
| 5 | 8 | 7102 | .014 |
| 2 | 4 | 7367 | .125 |
| 3 | 5 | 7693 | .042 |

¹Calculated from the molecular parameters listed in A. Lofthus and P.H. Krupenie, J. Chem. Phys. Ref. Data 6, 113 (1977).

²Calculations done by W. Benesch and K. Saum, J. Phys. B 4, 732 (1971).

Table VIII

Frank-Condon Factor

| <u>w-a</u> | | <u>w-X</u> | | <u>X+w+a</u> |
|------------|-------|------------|-------|--------------|
| 0-0 | .6842 | 0-0 | .0031 | .002 |
| 1-1 | .2662 | 0-1 | .014 | .004 |
| 2-2 | .0714 | 0-2 | .035 | .003 |
| 3-3 | .005 | 0-3 | .061 | .0003 |
| 4-4 | .006 | 0-4 | .087 | .0005 |
| 5-5 | .035 | 0-5 | .106 | .004 |
| 6-6 | .073 | 0-6 | .113 | .008 |

$0.1 \text{ cm}^{-1}/760 \text{ torr}$ or $3 \times 10^9 \text{ Hz}/760 \text{ torr}$ for various infrared lines. If we accept the collision frequency of 10^5 Hz at 0.1 torr , the vibrational quenching would occur at a rate of 10^{-5} sec at 0.1 torr . Anyway, either estimate for the $X N_2$ quenching is found quite faster than the radiative lifetime of the $w^1\Delta$ state.

The intrasystem cascading process discussed by Saum and Benesch⁹ would be applicable for the $w-a$ transition. The situation for this case is much more straightforward than the triplet transition discussed by them. It is because the singlet transition $w-a$ is isolated from other companion transitions, while the $W-B$ transition is intimately connected to the $B-A$ transition. The intrasystem cascading process occurs to allow downward electronic transitions within the system when the arrays of vibrational levels are mutually interspersed in the two electronic states connected by the transition in question. Our situation is distinguished from the case discussed by Saum and Benesch in that the electronic transitions in the intrasystem cascading are predominantly collision-induced, thus the photon emission being suppressed. The intersystem cascading contributes to populate the bottom levels in the vibrational ladder, while the released energy in the intrasystem cascading would be effectively transferred to the $X N_2$ by the collisional process. The $v = 0$ levels of both the $w^1\Delta$ and $a^1\pi$ state are populated at an excessive rate. The lower state is depleted at a faster rate by the $a^1\pi - X^1\Sigma$ transition than the upper state, thereby establishing the population inversion at the $v = 0$ levels. Our source configuration of a 36-meter long path would contribute to achieve a large gain in the super-radiant emission.

The Transitions Between the Triplet States

The (2-0) band centered at 3008 cm^{-1} was the only W-B transition observed in our data. Even though the band is contaminated by two N I lines, the band exhibited an excessively high intensity. Application of a simple calculation similar to the one done for the w-a transition led us nowhere in explaining why the (2-0) band was so special for achieving the unusually high intensity.

As mentioned earlier, we observed an extremely unstable behavior of the B-A transition. We failed to find any relations relating the pressure, the current density, and other parameters to the emission of both the W-B and B-A transitions. The resident time of the molecules in the discharge span is rather long; an order of 10^4 discharge cycles. The end products of the transitions involving the triplet states are the $A^3\Sigma$, which are normally deactivated by the collisional process with the ground state nitrogen ($X^1\Sigma$). Taking a value of 10^{-4} for the triplet state production rate per a single discharge cycle, and the average resident time mentioned above, we estimate that a substantial portion of the N_2 molecules would stay up either in the $A^3\Sigma$ state or in the high v levels of the $X^1\Sigma$ state, as an equilibrium is established under the glow discharge condition. The excitation energy attained by these states cannot be released quickly because no photon releases are allowed in the process for bringing these molecules to the ground state. One would expect that the B-A transition is affected by the condition established in the equilibrium.

Our data indicated that the equilibrium was not established uniquely as demonstrated by the extremely unstable emission intensity of the B-A transition. As a hindsight, we should have been able to cure the

condition by implementing a much faster flow to the gas sample than what we had.

No calculations were carried out to estimate the population density of various N_2 excited states, partly because we were skeptical of the $W^3\Delta$ state as proposed by Benesch and Saum. Our skepticism was based on the abnormal intensity pattern in the vibrational progression of the W-B transition. In the most recent work, Verges and his co-workers completed a detailed spectral analysis of 19 vibrational bands of the W-B transition,²¹ confirming the original assignment of Benesch and Saum. Now that our skepticism is cleared, we are ready to proceed with a theoretical computation to see whether the emission pattern observed in our data can be demonstrated.

References

1. G. Vanasse and H. Sakai, "Fourier Spectroscopy" in Progress In Optics, Vol. VI, Ed. E. Wolf, North-Holland, Amsterdam (1967).
2. D.J. Lovell and J. Strong, *Appl. Opt.* 8, 1673 (1969).
3. The most recent data compilation for infrared atomic lines by M. Outred, *J. Chem. Phys. Ref. Data* 1, 1 (1978) contains no data of these atomic lines.
4. Comprehensive data for N₂ are compiled by A. Lofthus and P.H. Krupenie, *J. Chem. Phys. Ref. Data* 6, 113 (1977).
5. For the recent energy data compilation, see M. Mizushima, The Theory of Rotational Diatomic Molecules, Wiley, NY (1975).
6. P.H. Krupenie, *J. Chem. Phys. Ref. Data* 1, 423 (1972).
7. C.E. Moore, NSRDS-NBS 3, Sect. 7, U.S. Government Publication (1976).
8. G.H. Dieke and D.F. Heath, Johns Hopkins Spectroscopic Report, The Johns Hopkins University, Baltimore MD (1959).
9. W. Benesch and K. Saum, *J. Phys. B* 4, 732 (1971).
10. R.A. McFarlane, *Phys. Rev.* 146, 37 (1966).
11. J.P. Maillard, J. Chanville and A.W. Mantz, *J. Mol. Spec.* 63, 120 (1976).
12. R.N. Dixon, *Can. J. Phys.* 37, 1171 (1959).
J. Malicet, J. Brion and H. Guenebaut, *J. Chem. Phys. (Fr.)* 67, 25 (1970).
13. I. Hansen *et al*, *Chem. Phys. Ltrs* 42, 370 (1976).
J. Mulvihill *et al*, *Chem. Phys. Ltrs* 35, 327 (1975).
14. C. Amiot, Dissertation, l'Université Pierre et Marie Curie (1976).
15. R.A. McFarlane, *IEEE J. Quant. Elect.* 2, 229 (1966).
16. C. Effantin *et al*, *J. Mol. Spec.* 76, 221 (1979).
17. W. Benesch and K. Saum, *J.Q.S.R.T.* 12, 1129 (1972).
K. Saum and W. Benesch, *Appl. Opt.* 9, 1419 (1970).
18. C. Effantin *et al*, *J. Mol. Spec.* 76, 204 (1979).

19. D.C. Cartwright *et al*, Phys. Rev. A 16, 1041 (1977).
20. D.C. Cartwright, J. Geophys. Res. 83, 517 (1972).
21. E. Cerny, F. Roux, C. Effantin, J. D'Incan and J. Verges, J. Mol. Spec. 81, 216 (1980).

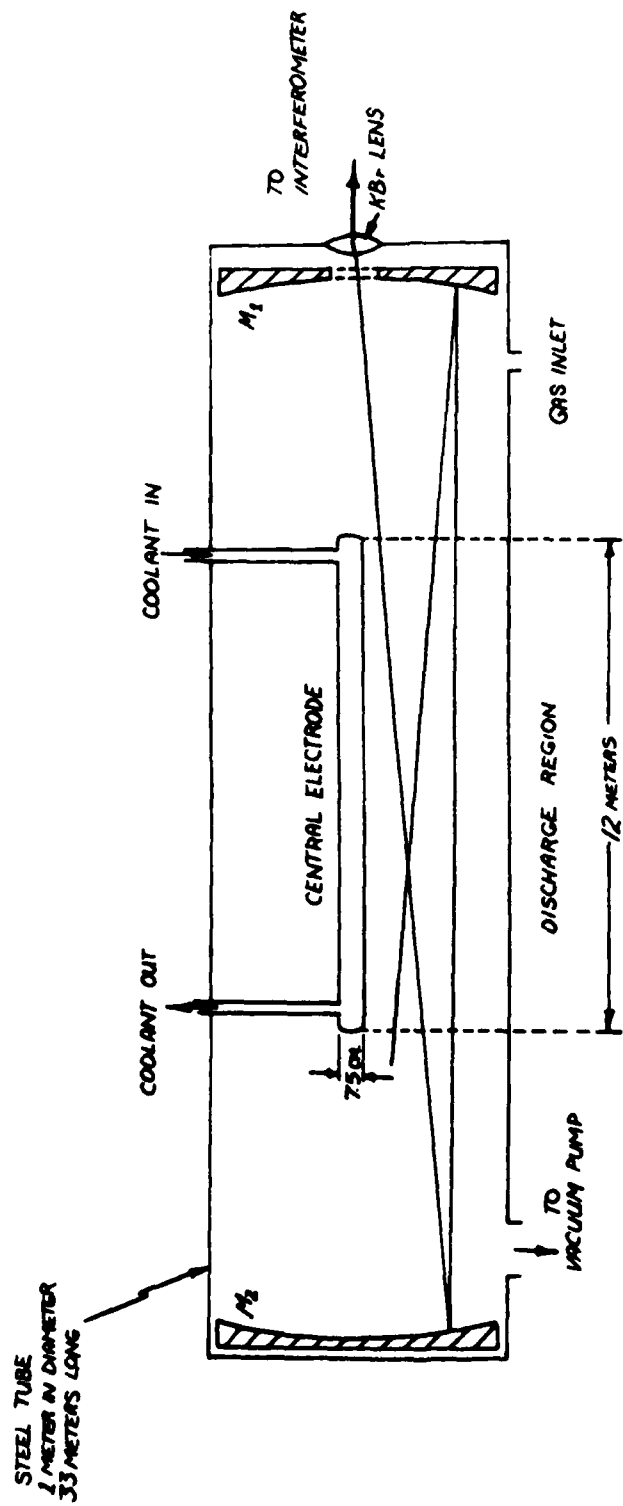


Fig. 1 SCHEMATIC REPRESENTATION OF THE DISCHARGE COLUMN (NOT TO SCALE). MIRRORS M₁ AND M₂ ARE FOCUSED ON EACH OTHER RESULTING IN THREE PASSES THROUGH THE DISCHARGE COLUMN.

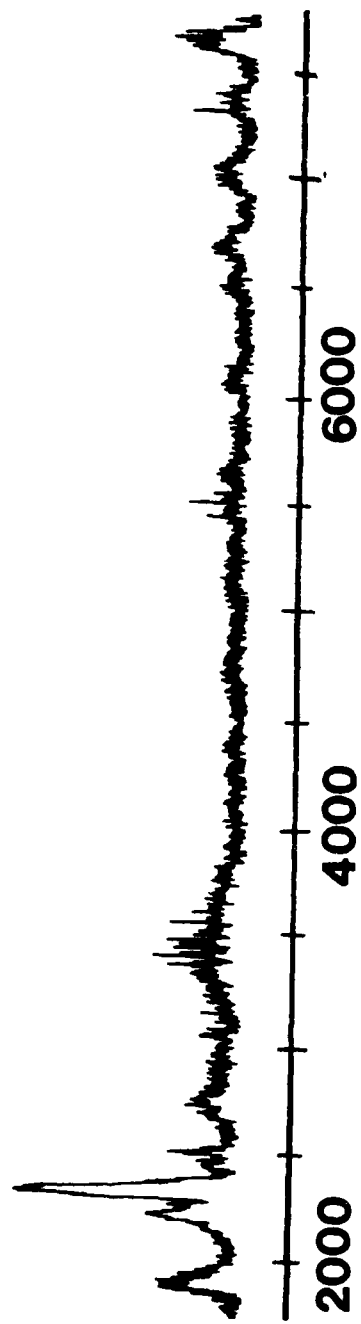


FIG. 2 Glow discharge spectrum of air.

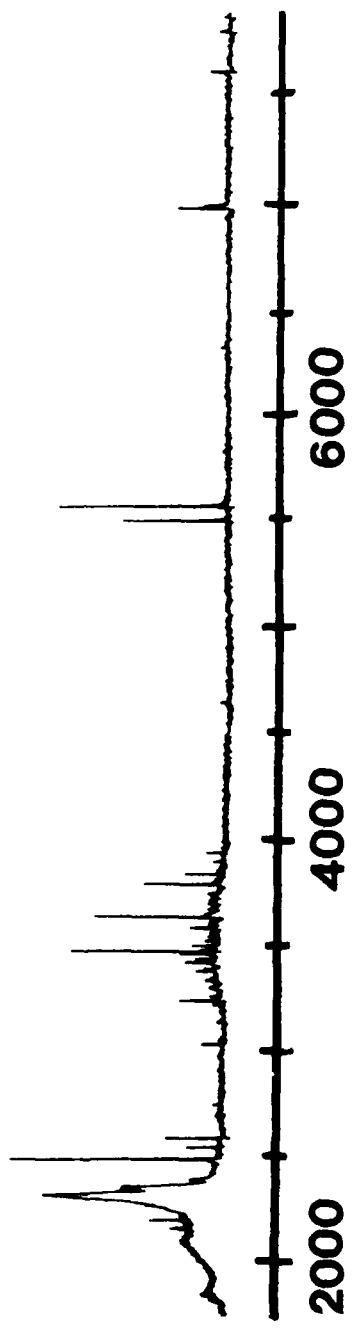


Fig. 3 Glow discharge spectrum of O₂.

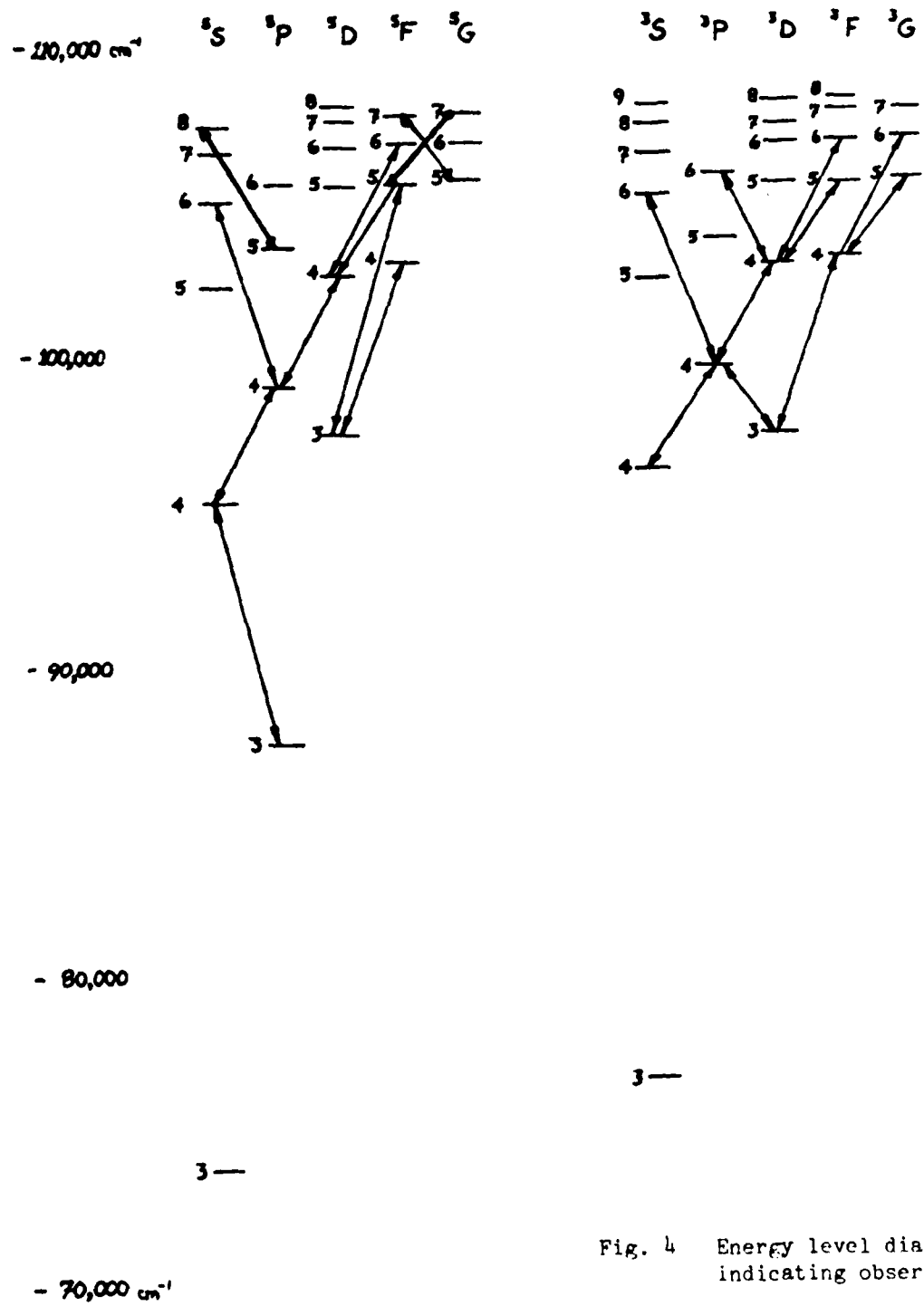


Fig. 4 Energy level diagram of atomic O I indicating observed transitions.

$$2S^1 2P^3 \quad ^3P_1 = 0.0 \text{ cm}^{-1}$$

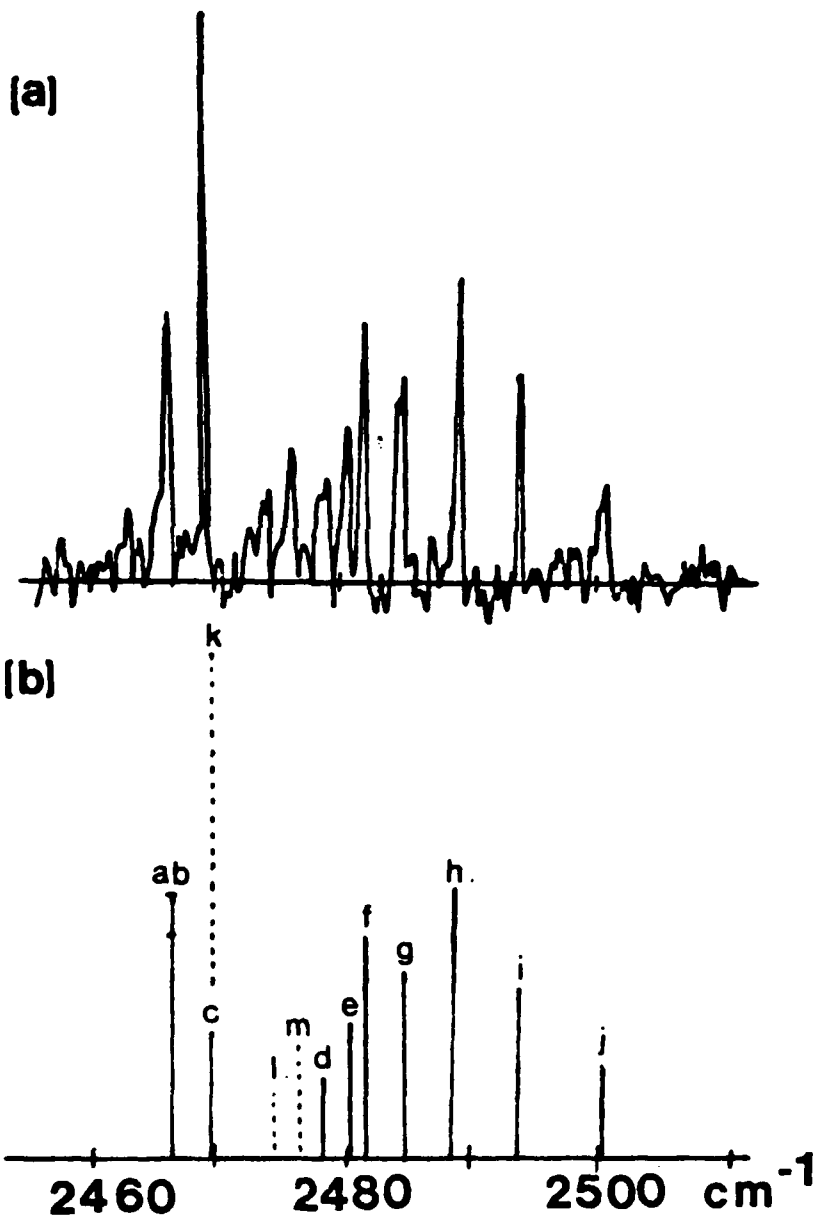


Fig. 5
(caption on next page)

Figure 5(a) The observed spectrum between 2455 and 2505 cm^{-1} .

Figure 5(b) Identification of the spectral lines.

N I lines, a: $j=2$ $K= 3\leftarrow 3$

b: $j=2$ $K= 4\leftarrow 5$

c: $j=2$ $K= 3\leftarrow 4$

d: $j=2$ $K= 2\leftarrow 3$

e: $j=1$ $K= 2\leftarrow 3$

f: $j=1$ $K= 4\leftarrow 5$

g: $j=0$ $K= 3\leftarrow 4$

h: $j=2$ $K= 5\leftarrow 6$

i: $j=1$ $K= 3\leftarrow 4$

j: $j=2$ $K= 1\leftarrow 2$

He I lines, k: $4f^1F\leftarrow 5g^1G$ and $4f^3F\leftarrow 5g^3G$

l: $4d^1D\leftarrow 5f^1F$

m: $4d^3D\leftarrow 5f^3F$

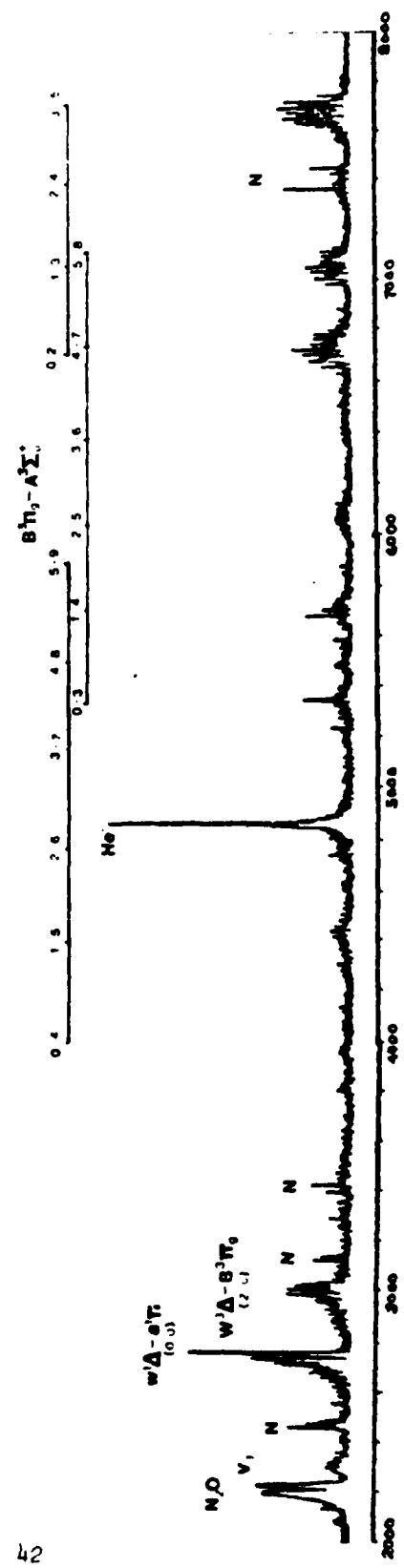


Figure 6 Observed electronic transitions of molecular and atomic nitrogen.

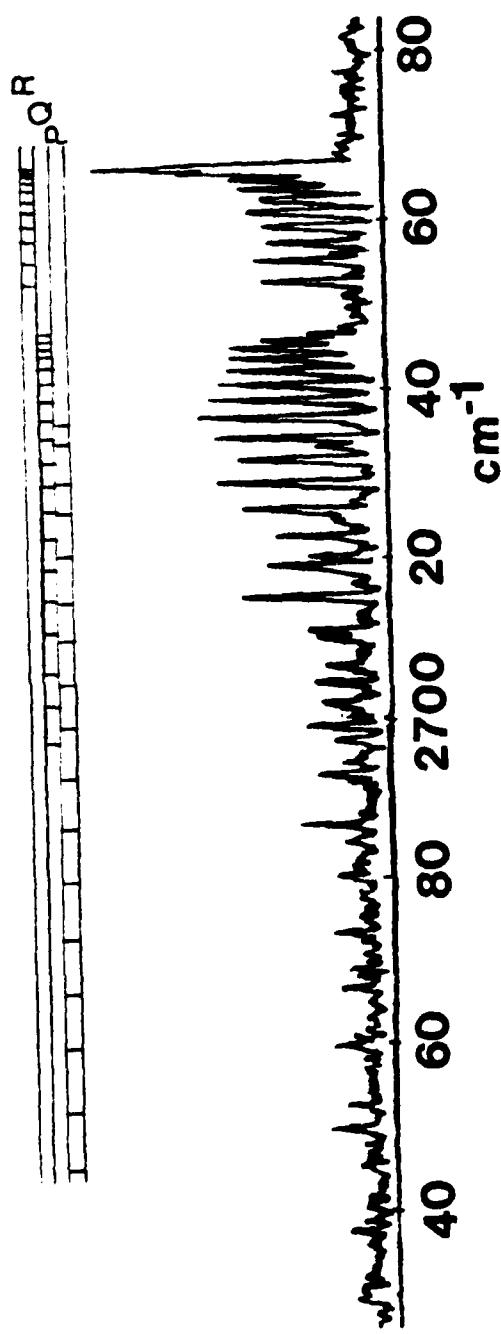


Fig. 7 Spectrum of the $v_1^1 \Delta - e_1^1 \pi$ (0-0) transition.

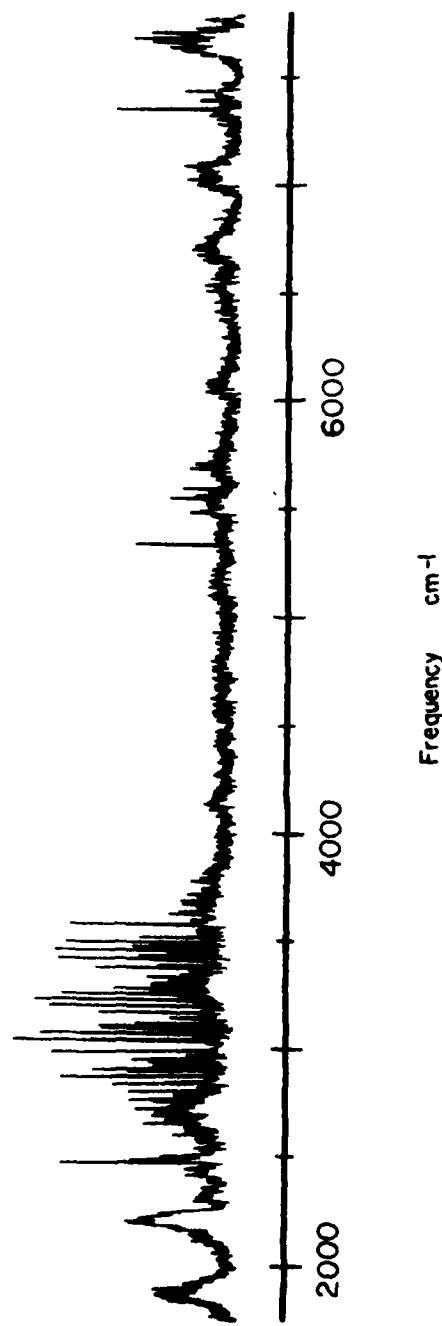


Fig. 8 Glow discharge spectrum of air mixed with H₂.
Mixture ratio: air 3 and H₂ 1.

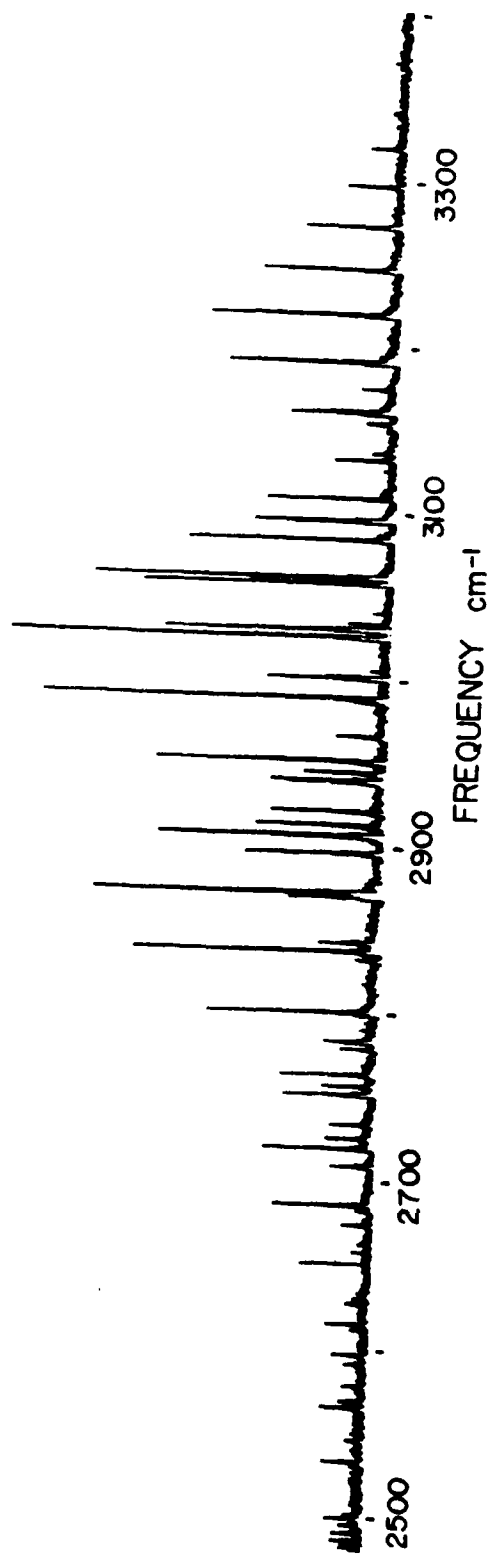


Fig. 9 Infrared spectrum of NH (3R);
spectral resolution 0.12 cm^{-1} .

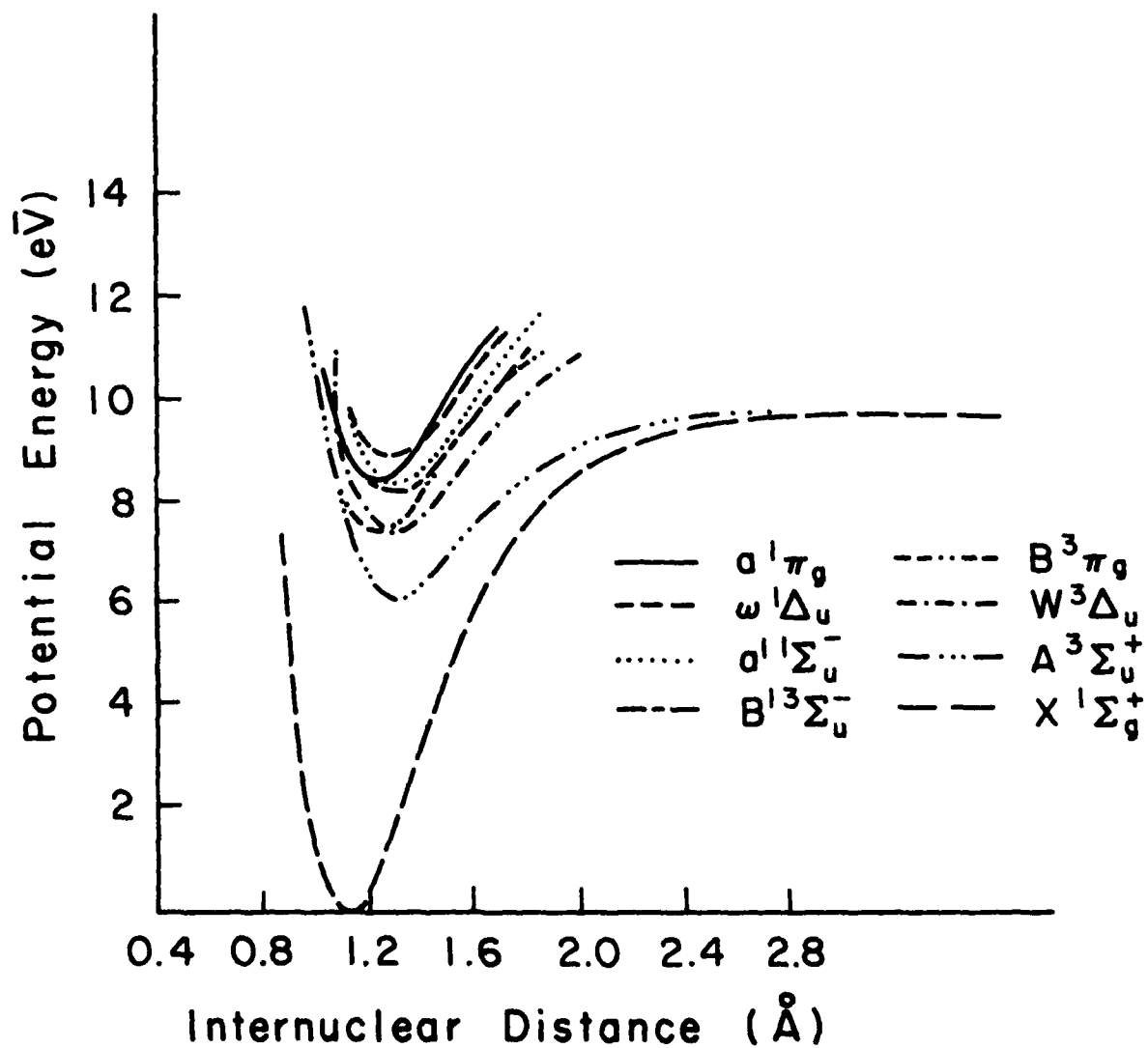


Fig. 10 Potential curves of N_2 .

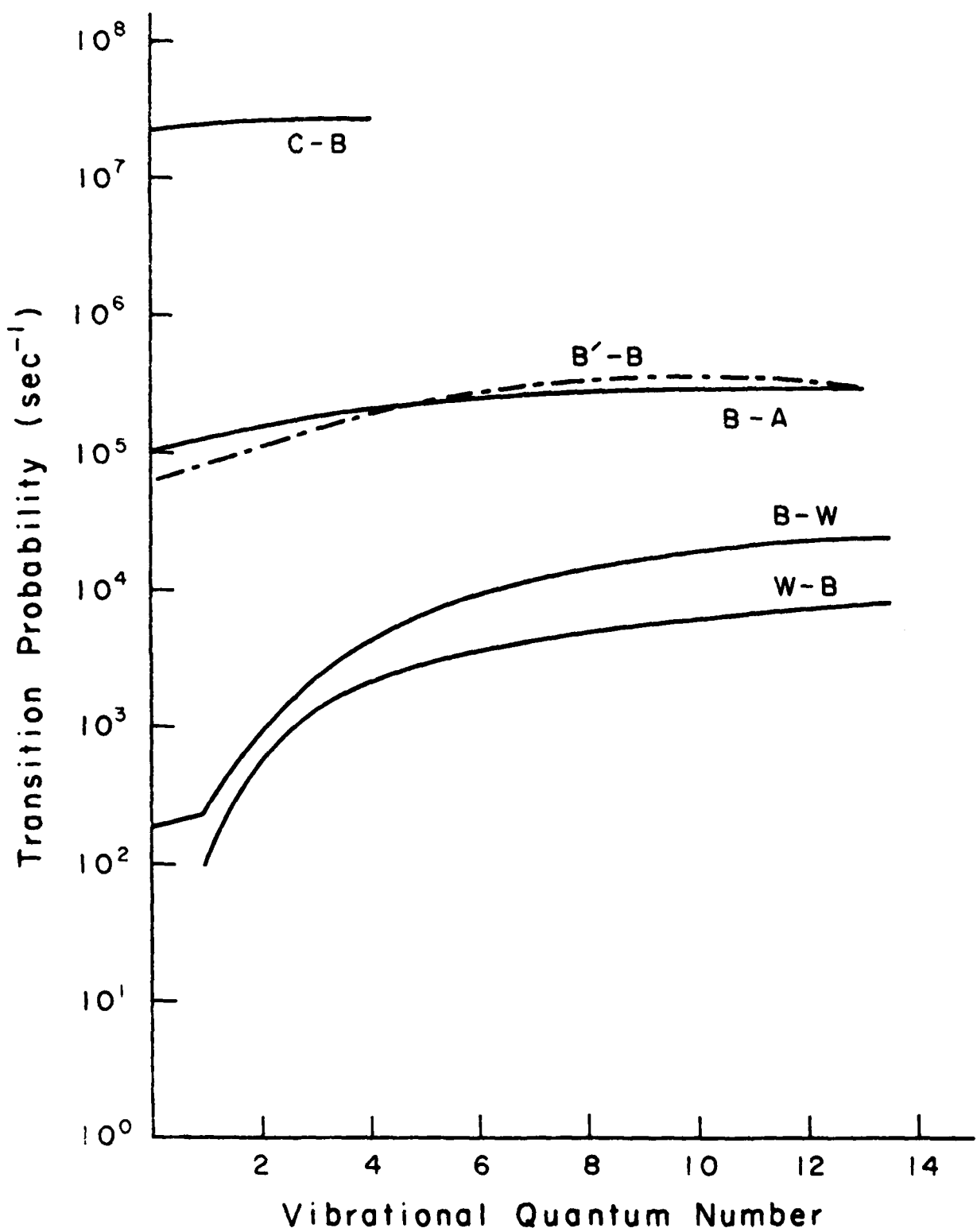


Figure 11a, Transition probabilities of N_2 , triplet states.
 D.C.Cartwright, J. Geophys. Res. 83 517 (1978)

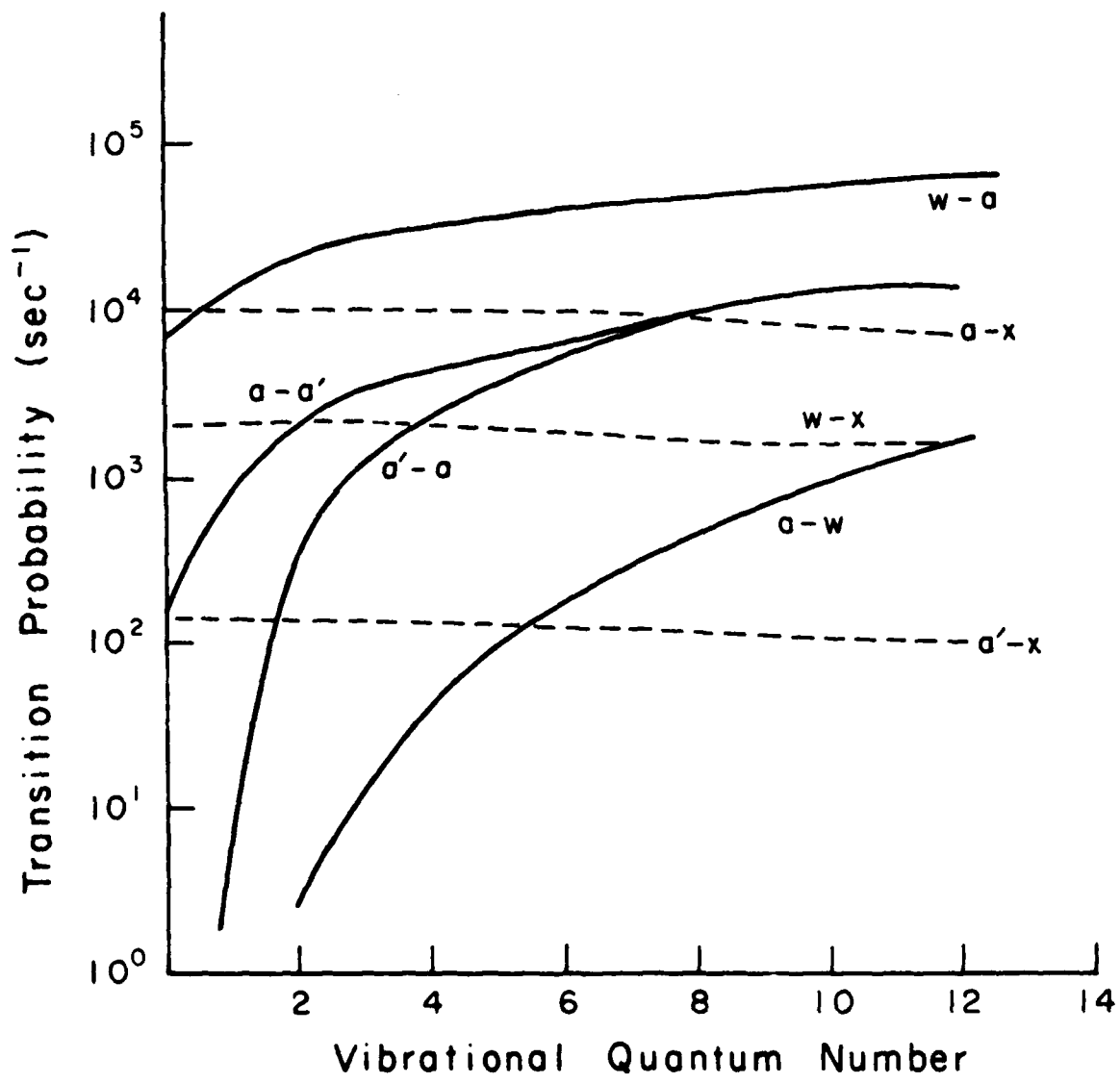


Figure 11b, Transition probabilities of N_2 , singlet states.
 D.C. Cartwright, J. Geophys. Res. 83 517 (1978)

END
DATE
FILMED
10-81
DTIC